[Manuscript]

Comparing the effects of internal stem damage on aboveground biomass estimates from terrestrial laser scanning and allometric scaling models

Running head: Internal stem damage and tree aboveground biomass

Abstract

1. Forests and woodlands are critical carbon stores, and methods for quantifying forest aboveground biomass (AGB) are increasingly relied upon for determining sequestered CO_2 traded in carbon markets. AGB is traditionally measured using allometric models, yet terrestrial laser scanning (TLS) is emerging as a highly accurate remote sensing alternative. However, internal tree stem damage from biotic decay is an unresolved source of error for both TLS and allometries, with implications for accurate carbon assessment.
2. We destructively harvested 63 TLS-scanned trees in an Australian savanna to understand the impact of internal damage on AGB estimation at individual tree- and plot-levels. We tested the performance of TLS versus five allometries in measuring AGB, applying both database and field-measured wood specific gravity. We recorded how internal damage changed throughout the tree and tested if tree size and internal stem damage amount contributed to AGB under or over predictions.
3. We asked four questions: 1) How accurately does TLS measure AGB in comparison to allometries at both tree- and plot-levels? 2) Does applying field-measured or database wood specific gravity values affect TLS and allometry AGB estimate accuracy? 3) How does internal stem damage vary throughout trees? 4) Does tree size or amount of internal stem damage predict AGB overestimation?
4. TLS provided closest estimates to aggregated AGB at the plot-level. At the tree-level, all methods were strong at predicting field-measured AGB (R^2>0.84), however we found TLS using field-measured wood specific gravity to be most accurate (R^2=0.99). Although allometric models were unaffected by internal damage, TLS tended to overpredict AGB of

large, damaged trees. Roughly half of the trees in the study sustained 1-10% damage, which was most extensive at the base and main trunk, decreasing into the crown.

5. *Synthesis and applications:* For plot-level forest carbon estimation where internal stem damage is low (<10%), we recommend TLS to accurately estimate AGB, as well as in situations where precision is required at the individual tree-level. When quantifying AGB using TLS in more damaged wooded ecosystems (>10%), internal stem damage should be quantified to avoid overestimation and maintain high standards of precision in carbon markets.

Keywords

Allometric models, forest carbon credits, internal tree stem damage, terrestrial laser scanning, tree aboveground biomass

Introduction

Forests and woodlands are critical global carbon (C) stores, absorbing atmospheric carbon dioxide (CO_2) which is sequestered as tree biomass or passed into detrital and soil C pools (Pan et al., 2011; Pörtner et al., 2022). As the Earth's climate warms due to excess C in the atmosphere, natural C sinks such as trees are potential, yet debated, resources for mitigation (Bastin et al., 2019), but see (Veldman, 2019). Globally, forest C stocks are estimated to store 861 ± 66 Pg C, more than half of which is in tropical forests (Pan et al., 2011). These global estimates of tree C are derived from scaling up local plot biomass inventories, so it is critical to accurately quantify individual tree C stored as aboveground biomass (AGB).

Accuracy of AGB estimates at the plot level is important for understanding terrestrial carbon stocks, and precise measurement of individual trees is also necessary for determining critical questions in forest ecology such as tree allocation patterns. For example, AGB distribution among species, crown to stem ratios and tree sizes rely on accurate measurements from individual trees (Burt et al., 2021; Xing et al., 2019). Similarly, comprehensive characterization of the structural distribution of tree AGB is a fundamental indicator of ecological condition (Eyre et al., 2015). It is therefore important that sources of error in calculating AGB are identified and addressed. Without an understanding of estimation errors, we risk making misinformed decisions in the management of natural C storage processes.

Internal stem damage alters the C stored in trees and is especially prevalent in savanna ecosystems where termites, wood-decomposing fungi and fire interact, leading to high proportions of 'missing' biomass in living trees (Adkins, 2006; Flores-Moreno et al., 2023; N'Dri et al., 2011; Perry et al., 1985; Werner & Prior, 2007). Internal stem damage, here defined as decomposition of tree heartwood and sapwood, is hypothesized to be a natural part of some species' life history (Janzen, 1976; Ruxton, 2014). Previous studies identified internal stem damage from single points or cross-sections near the base of trees (I. F. Brown et al., 1995; Eleuterio et al., 2020; Werner & Prior, 2007; Zeps et al., 2017). The few studies that tested for implications of internal damage on AGB and C storage found that internal stem damage ranged between 7% and 42% in tropical ecosystems around the globe (Flores-Moreno et al., 2023; Heineman et al., 2015; Monda et al., 2015). However, for most forest and woodland ecosystems there is limited information about the extent of internal damage; further, widely used biomass and C models largely do not explicitly quantify this source of error. If trees are assumed to be solid structures, it is expected that high levels of internal stem damage would lead to overestimated forest C.

To assess the amount of biomass in trees, traditional research methods use allometric scaling models (ASMs) that define relationships between tree attributes such as diameter at breast height (DBH), crown height, and wood specific gravity (oven dry mass/green volume (g cm^{-3})) to predict AGB. Wood specific gravity can be measured in the field from the same population of trees as measured for DBH and height, or sourced from reference databases such as Zanne et al. (2009). Wood specific gravity values can be variable within and among species and at different spatial scales, so field-measured values from a specific site are likely to be most accurate (Sæbø et al., 2022). Additionally, reference database wood specific gravity values are often associated with millable lumber in forestry, and tend to be biased toward heartwood at the tree base where sampling is more accessible (Wassenberg et al., 2015). Ultimately, ASMs and wood specific gravity are used to estimate AGB and can then be converted to C content for C accounting, as wood is generally ~50% C by dry weight (Martin et al., 2018).

The equations underlying ASMs are informed by destructive-harvest studies (S. Brown, 1997; Ketterings et al., 2001), and while ASMs are widely used to estimate forest AGB, they have several limitations. First, the models are not universally applicable as they are usually specific to geographic or climatic regions, or to specific tree species (Henry et al., 2013; Pillsbury & Kirkley, 1984). Although efforts have been made to develop universally applicable ASMs, which have been widely adopted (Chave et al., 2014), the destructive harvest data underlying them are not replicated for all species and ecosystems. Importantly, ASMs can capture internal stem damage if underlying destructive harvest data include damaged trees (Monda et al., 2015), but ASMs used in ecosystems with different amounts of damage may produce inaccurate AGB estimates. Furthermore, large trees are often underrepresented in the datasets used to generate ASMs (Chave et al., 2014), despite comprising a disproportionate amount of forest biomass (Slik et al., 2013). ASMs have been shown in one study to overestimate AGB for larger trees (Burt et al., 2021). Finally, while crown biomass is estimated as it scales with measurements of height and DBH, ASMs fail to capture variation in crowns and general canopy structure (Ploton et al., 2016). For these reasons, two ASMs even when designed for the same location may generate different AGB estimates (Chave et al., 2005). Due to these limitations, a push for more rapid, size unbiased, and accurate tree biomass estimates over larger areas has led to a rise in the use of remote sensing technologies such as Light Detection and Ranging (LiDAR), a method of measuring forests that has the potential to facilitate more accurate volume estimates which improve in turn AGB and forest C estimates.

Increasingly, new technologies such as Terrestrial Laser Scanning (TLS) are being used to measure forest AGB. TLS is a type of ground-based LiDAR that generates mm-resolution reconstructions of tree volumes, from the individual level (Burt et al., 2021) up to entire forest stands (Calders et al., 2015; Momo Takoudjou et al., 2018). Tree AGB can then be estimated by multiplying TLS-generated tree volumes by wood specific gravity. The accuracy of TLS has been tested using destructive harvest studies in which living trees are scanned and destructively harvested to validate biomass estimates. Demol et al. (2022) reviewed ten TLS destructive harvest studies, comprising 391 trees from 111 species across a global range of ecosystems, to demonstrate that TLS is an accurate tool for estimating tree biomass at large scales. However, it was noted that AGB estimations for smaller trees (<1000 kg) were inflated due to over-modeling of tree volume (Demol et al., 2022). In contrast, for larger trees (>3,900 kg), Burt et al. (2021) found that TLS error did not increase with tree size. As TLS does not require the regional calibration as in high-performing ASMs, it has the potential to provide a more unbiased measure of forest AGB at broad landscape scales and can serve as a substitute for calibrating ASMs (Momo Takoudjou et al., 2018). However, despite its proven accuracy TLS is unable to detect or estimate the amount of internal stem damage present in trees (Demol et al., 2022).

Current lack of clarity around the frequency and severity of internal stem damage in forest and woodland ecosystems extends to our understanding of how internal stem damage is distributed throughout a tree and the extent to which the distribution depends on biotic and abiotic factors. For example, microbes and termites that cause internal decay often enter trees at the base (Adkins, 2006; Perry et al., 1985), which may lead to the greatest damage near the entry points relative to tree canopies. In some ecosystems, including tropical rainforests and Australian savannas, termites in the genus *Coptotermes* cause extensive internal stem damage, removing large amounts of heartwood to form 'pipes' (Apolinário & Martius, 2004; Werner & Prior, 2007) that extend into the canopy. However, internal damage may not occur consistently across trees; measurements through the tree are needed to determine the distribution and degree of internal damage, and how that damage impacts AGB and C estimates.

Here we carry out a destructive harvest study in Far North Queensland (FNQ), Australia in a savanna woodland ecosystem with a known prevalence of internal stem damage (Flores-Moreno et al., 2023) and termite mounds (Frith & Frith, 1993), adding a new monsoonal tropical ecosystem to the growing global database of TLS validation studies. We provide the first dataset combining TLS and ASMs with field-measured biomass and quantification of internal stem damage extent and distribution. We sought to answer four main questions: 1) How accurately does TLS measure AGB in comparison to allometries at both tree- and plot-levels? 2) Does applying field-measured or database wood specific gravity values affect TLS and allometry AGB estimate accuracy? 3) How does internal stem damage vary throughout trees? 4) Does tree size or amount of internal stem damage predict AGB overestimation? We expected TLS to capture AGB with higher accuracy than ASMs, and application of field-measured wood specific gravity to provide AGB estimates with highest accuracy. We also predicted that damage in trees would be greatest at the tree base, that small trees would contribute disproportionately to TLS overestimates of AGB, and that high levels of damage at the tree-level would lead to greater AGB overestimates from TLS.

Materials and Methods

Study site

The study was carried out in October 2022 in the Iron Range (Kutini-Payamu) on Cape York Peninsula, Far North Queensland (-12.7781, 143.3199). The Iron Range is a hilly coastal region of the Australian Monsoon Tropics 530 km northwest of Cairns, with a wet–dry tropical climate. The majority of annual rainfall (mean = 2057 mm, range = 1119−3299 mm (Australian Bureau of Meteorology, 2023)) is between December and April, and mean annual temperature = 26°C with a monthly average daily temperature range between 20.6 and 30.9 °C. The site is a pyrogenic savanna of *Corymbia clarksoniana* and *C. tessellaris* (Myrtaceae) open forest on metamorphic coastal ranges, and is surrounded by endemic mesophyll/notophyll vine forest on metamorphic slopes and plateaus (Queensland Regional Ecosystems 3.11.5 & 3.11.1 (Neldner et al., 2017)). Other dominant species within the savanna include *Eucalyptus tetrodonta*, *Lophostemon suaveolens* (Myrtaceae) and *Parinari nonda* (Chrysobalanaceae), with a sparse subcanopy of *Planchonia careya* (Lecythidaceae), *Grevillea parallela* (Proteaceae) and *Acacia flavescens* (Fabaceae). We capitalized on a pre-planned tree clearance to form a firebreak on two survey areas (lower 1.84 ha, upper 0.27 ha) (Fig. 1). These areas had a mean stem density of 326 trees ha^{-1} and a TLS-modelled DBH range of 1.3 to 69.7 cm (mean = 17.1 cm, standard deviation (SD) = 12.1 cm, Supplementary Fig. 5).

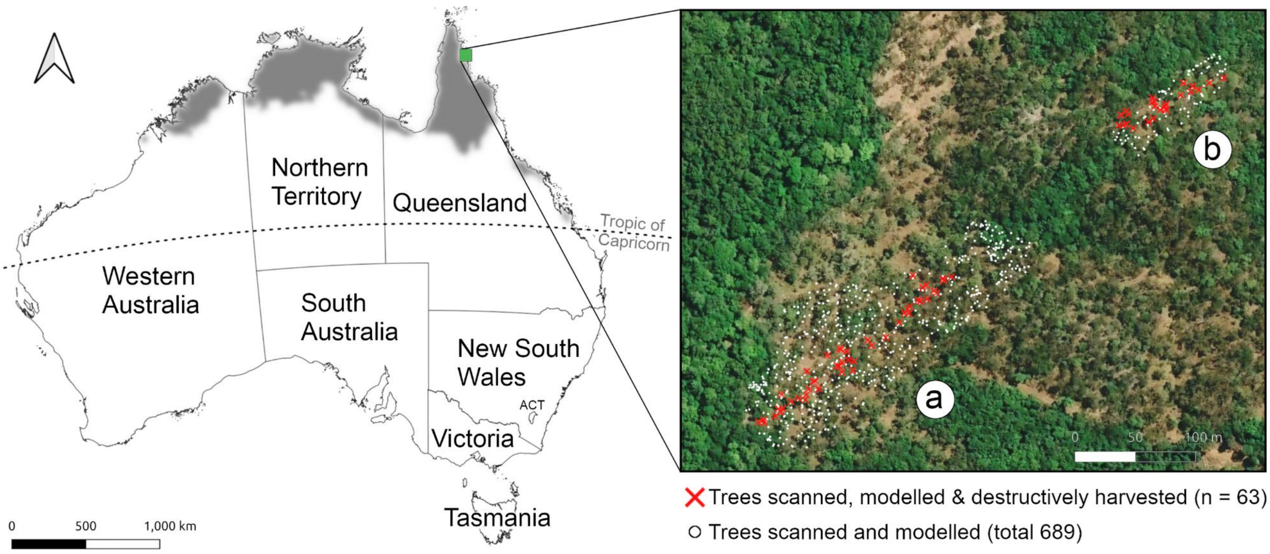

Figure 1 Study area. Left: Australian tropical savanna (grey, Köppen-Geiger climate classification Aw, (Beck et al., 2018) spans the northern tips of the Northern Territory, Western Australia and Queensland, where the study area is located (denoted with a green square) on Cape York Peninsula. Right: TLS scan areas in lower (a) and upper (b) survey areas showing destructively harvested trees (red) and all other trees (white) that were scanned and modelled.

Terrestrial laser scanning and point cloud processing

The study site overlaps with an existing long-term TLS survey area. TLS scanning was carried out for the two firebreak survey areas on 12 July 2022. One hundred and forty scans (lower survey area 111; upper survey area 29) in grid layout with 10 m spacing were collected using Riegl VZ-400i Laser Scanners (RIEGL Laser Measurement Systems, Horn, Austria) on the Pano-40 setting (Supplementary Fig. 4). TLS maps structures, such as trees, in three dimensions by emitting a laser pulse and measuring the time taken for light to return once reflected by the surface of measurement (Lemmens, 2011). Distances are inferred based on reflectance time which gives positional information, known as ‘point clouds’ used to reconstruct the entire structure of trees.

Point clouds were registered in RiSCAN Pro v2.14 and segmented using *treeseg* v0.2.2 (Burt et al., 2019). After segmentation, the tree point clouds were modelled using TreeQSM v2.4.1 (Raumonen et al., 2013) to generate cylinder models and estimate tree volume. Georeferenced field photos were used to confirm tree models. Desk audits were performed to manually check the accuracy of cylinder models against the point cloud, and poorly modelled trees were identified and reprocessed.

Destructive harvest protocol

Sixty-three trees within the firebreak survey area were felled with a chainsaw to compare field-measured biomass with TLS and ASM biomass estimates; 10 small trees with a mean DBH of 5.5 cm did not model correctly using TreeQSM. Felled trees were cut into main trunk segments and canopy branches for measuring field AGB using a 3T crane scale (SCS3000, Scintex, Eagle Farm, QLD, Australia) suspended from a Manitou telehandler (Manitou Group, Ancenis, France). Trunk segments were supported for mass measurements using slings, and canopy branches were weighed in a cargo net (2 × 2 m, 200mm mesh).

Cross-section samples

Thirty-nine trees with signs of internal damage at the base and/or first branching point were subsampled with four to seven cross-sections distributed at heights through the stem, with the number of sections dependent on tree height to maximize the diversity of diameter size classes (Supplementary Table 1, Fig. 2) and measure the vertical distribution of internal stem damage. As trees were of different sizes and architectures, we sampled the main stem segment (cut points C1 at the scarf felling point, C3 at the first main major branching point, and C2 midway between points C1 and C3) and then captured decreasing size classes into the canopy with ascending branching orders (C4 to C7). The largest cross-sections were taken at the scarf (C1), and the smallest at the canopy branches (C7). From individual tree quantitative structural models (QSMs), we used the diameter of cross sections to determine the relative height (as a percentage) of the cross section in the tree.

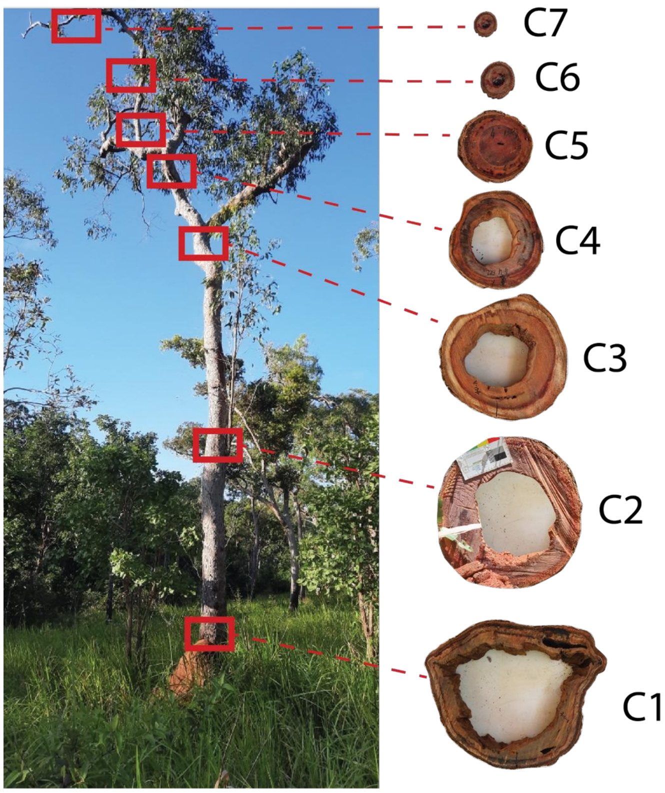

Figure 2 Cross-sectional sampling from tree base to canopy to quantify internal stem damage across a range of stem size classes (C1 largest, C7 smallest). See Supplementary Table 1 for further detail. Note presence of *Coptotermes* mound at base, which has been linked to occurrences of high internal stem damage from field observations. This was the most internally damaged tree in the study.

Cross-sections were placed in airtight plastic bags and stored in shaded areas in the field before transport back to the laboratory. Cross-sections were measured for green mass (m_{green}) and green volume (V_{green}) to represent field conditions. V_{green} was determined for each cross-section with the water displacement method on a balance measuring to the nearest 0.01 kg, and converted to volume assuming a density of water of 1.0 g cm^{-3}.

Each cross-section was photographed to quantify the proportion of damage, measured on an area basis using a shape area classifier in Adobe Illustrator (https://gist.github.com/bryanbuchanan/11387501). For each photo, total proportion damage (from both microbial and termite damage) was classified as the area of damage divided by the total area of the cross-sectional sample. Cross-section samples were held for less than one week at the field station laboratory before being dried at 105 °C to constant mass to determine dry mass

(m_{dry}) and water content (calculated as the difference between m_{green} and m_{dry}). We calculated wood specific gravity (p_{wood}) for each cross-section as m_{dry} / V_{green} (Panshin, AJ & De Zeeuw, C, 1980), which is commonly referred to as wood density in the literature (Zanne, Amy E., 2009; Zobel & Jett, 1995).

Species-level wood specific gravity

We examined wood specific gravity in two ways: field-measured and using a reference database. For field-measured wood specific gravity, we used cross-sectional samples with no internal stem damage from different positions in the tree (Table 1, Fig. 2). We tested if wood specific gravity changed throughout the tree using a linear mixed effect model (R package 'lme4') with cross section diameter (in cm) and species as predictors, individual tree as a random effect, and field-measured wood specific gravity as the response variable. As cross section size had no effect on wood specific gravity (Supplementary Table 10), field-measured wood specific gravity (p_{field}) at the species level was determined as average values across the undamaged cross section dataset for each species. To compare the performance of reference wood density (p_{ref}), we queried the Global Wood Density Database (Zanne, Amy E., 2009) for values for species in our study. For trees for which species-level information was not available, we used specific gravities of closest available relatives based on molecular phylogenies (Supplementary Table 2).

Quantifying internal damage from tree cross-sectional samples

We examined the relationship between diameter and internal damage using single-tree linear regression models for damaged trees with ≥ 3 cross-sectional samples. We applied this tree-specific relationship of size and damage to the cylinders comprising individual tree QSMs derived from TLS (Supplementary Fig. 3, Supplementary Table 5). For all cylinders in the model, we calculated the average internal damage of each cylinder based on its size, and then calculated overall tree internal damage as:

$$ISD_{tree} = \int_{1}^{C} V_{cyl.prop} * ISD_{lm} \qquad \text{(Eqn. 1)}$$

(where ISD_{tree} is overall tree internal stem damage, $V_{cyl.prop} = V_{cyl} / V_{tree}$, ISD_{lm} is internal stem damage given cylinder diameter (from individual tree-level estimate based on linear model regression predicting internal stem damage from diameter), and C = total number of cylinders in the tree QSM.

Calculating AGB from TLS

We used QSMs generated from TLS scans to determine tree volume (L), which was then multiplied by species-level p_{ref} and p_{field} to estimate AGB. All measurements in our analysis (for both TLS and ASMs discussed below) compared dry AGB, where field-measured green AGB was converted to dry AGB by multiplying m_{green} by average tree water content measured from its cross-sectional samples. We calculated TLS-estimated dry AGB for each tree by multiplying TLS tree volume (L) by wood specific gravity (for both p_{ref} and p_{field}). We define the comparison of a tree's estimated AGB with the individual tree field weight as 'tree-level' AGB model accuracy, and the aggregated, study-wide estimated AGB versus aggregated field-weighed AGB as 'plot-level' AGB model accuracy.

Calculating AGB from ASMs

To assess the performance of TLS against traditional methods of AGB estimation, we compared field-measured AGB with estimates derived from 5 published ASMs used in tropical forest biomass literature as well as Australian and global C markets (Supplementary Table 3). The ASMs by Paul et al. (2013), later refined by Paul et al. (2016), to distinguish between eucalypts and other tree types are widely used across Australia in the Full C Accounting Method (FullCAM (Richards & Brack, 2004)). Two global tropical ASMs, Brown (1997) and Chave et al. (2014), are used as gold-standard allometric equations for biomass, tropical C accounting in government and voluntary C markets, and REDD+ activities (Hirata et al., 2012). Allometries from Williams et al. (2005), Paul et al. (2016), Paul et al. (2013), and Brown (1997) require tree DBH as an input to calculate AGB. The model from Chave et al. (2014) requires p_{wood} and field-measured DBH as inputs, which we tested using both p_{ref} and p_{field} as described above. The Chave et al. (2014)

equation also includes a bioclimatic stress variable ‘E’, which combines temperature variability, precipitation variability, and drought intensity for a given location. This value, E for the study site was determined as 0.3687456 using site latitude and longitude in the R packages ‘raster’ and ‘ncdf4’ as demonstrated in Chave et al. (2014) (chave.ups-tlse.fr/pantropical_allometry.htm). AGB values were calculated using ASMs following Mascaro et al. (2011), adding standard error to regression coefficients *sensu* Baskerville (1972): standard error (SE) of the regression to the power of 2 divided by 2, i.e. =EXP(a + b × LN(*DBH*) + (SE^2)/2).

Correcting TLS and ASM biomass for unmeasured tree stumps

For trees that were felled above ground level (n = 38), we corrected AGB estimates to account for the stump biomass that remained in the ground. QSMs were cut at the scarf location with a custom Python script before densities were applied to generate accurate TLS volumes (Supplementary Data 1). ASMs for trees cut above ground level were corrected by calculating the volume of the stump using Smalian’s formula (where cylindrical volume is calculated by multiplying the average stump end area by stump height, (Köhl et al., 2006)), multiplying the resulting volume by p_{field} for a given tree, and subtracting the resulting weight from the ASM weight estimate.

Analyses

Estimating tree- and plot-level AGB using ASM and TLS

To test how well ASMs and TLS modelled individual tree biomass, we generated linear regression models with field-measured dry AGB as the predictor and ASM/TLS biomass as the response. We compared models based on their R^2 and residual standard error (RSE) values. We evaluated how each model (5 ASMs and TLS) predicted total AGB across the study area by comparing the percentage deviation from field-measured biomass for each model.

Internal stem damage throughout the tree

To assess the relationship between internal stem damage and height within the tree, we used linear mixed effect models with relative height of cross section (expressed as %) in the tree and as a fixed effect, and individual tree as a random effect, and percentage of internal damage as the log-transformed response.

Impact of internal stem damage on AGB estimates from TLS and ASMs

To test if TLS and ASMs overestimated the field-measured AGB of internally damaged trees, we calculated per-tree residuals (for both TLS and the Chave (2014) ASM) as TLS/ASM-predicted AGB values minus field-measured biomass and divided by field-measured biomass to normalize for tree size. We ran a linear regression with percentage of internal damage as a predictor with an interaction with DBH and residuals as the response (for both TLS and the Chave (2014) ASM), expecting that if TLS and the Chave (2014) ASM overestimated true AGB, residual values would be positive. We performed all analyses using R v4.2.3 (R Core Team, 2013).

Results

Estimating AGB using ASM and TLS for individual trees

Trees in the study had AGB ranging from 2.9 kg to 3056 kg (mean = 293 kg, SD = 544 kg, N = 63, Fig. 3). All ASMs and TLS gave strong predictions of field-measured AGB (R^2 > 0.84, Table 1) but TLS using p_{field} provided the most accurate estimates (RSE = 49.9 kg, R^2 = 0.991, Fig. 3c, Table 1, see Supplementary Fig. 1 for all ASM comparisons). The TLS model had an RSE approximately one-third of the best performing ASM model by Chave et al. (2014) using p_{field} (RSE = 161.7 kg, R^2 = 0.914, Fig. 3b, Table 1). The ASM model from Paul et al. (2016) provided the next best prediction of field-measured AGB (RSE = 189.2 kg, R^2 = 0.843, Fig. 3a, Table 1)

Estimating aggregated AGB using ASMs and TLS

When we compared the sum of dry tree AGB estimates across 63 trees, the estimate closest to the total field-measured AGB of destructively-harvested trees (18,438 kg) was from TLS using p_{field} (18,546 kg, +0.59% over total field-measured AGB, Supplementary Table 8). Accuracy of plot-level estimates from ASMs ranged from +12.3% over (Williams et al., 2005) to -27.1% under (Paul et al., 2013) (Supplementary Table 8, Fig. 3d).

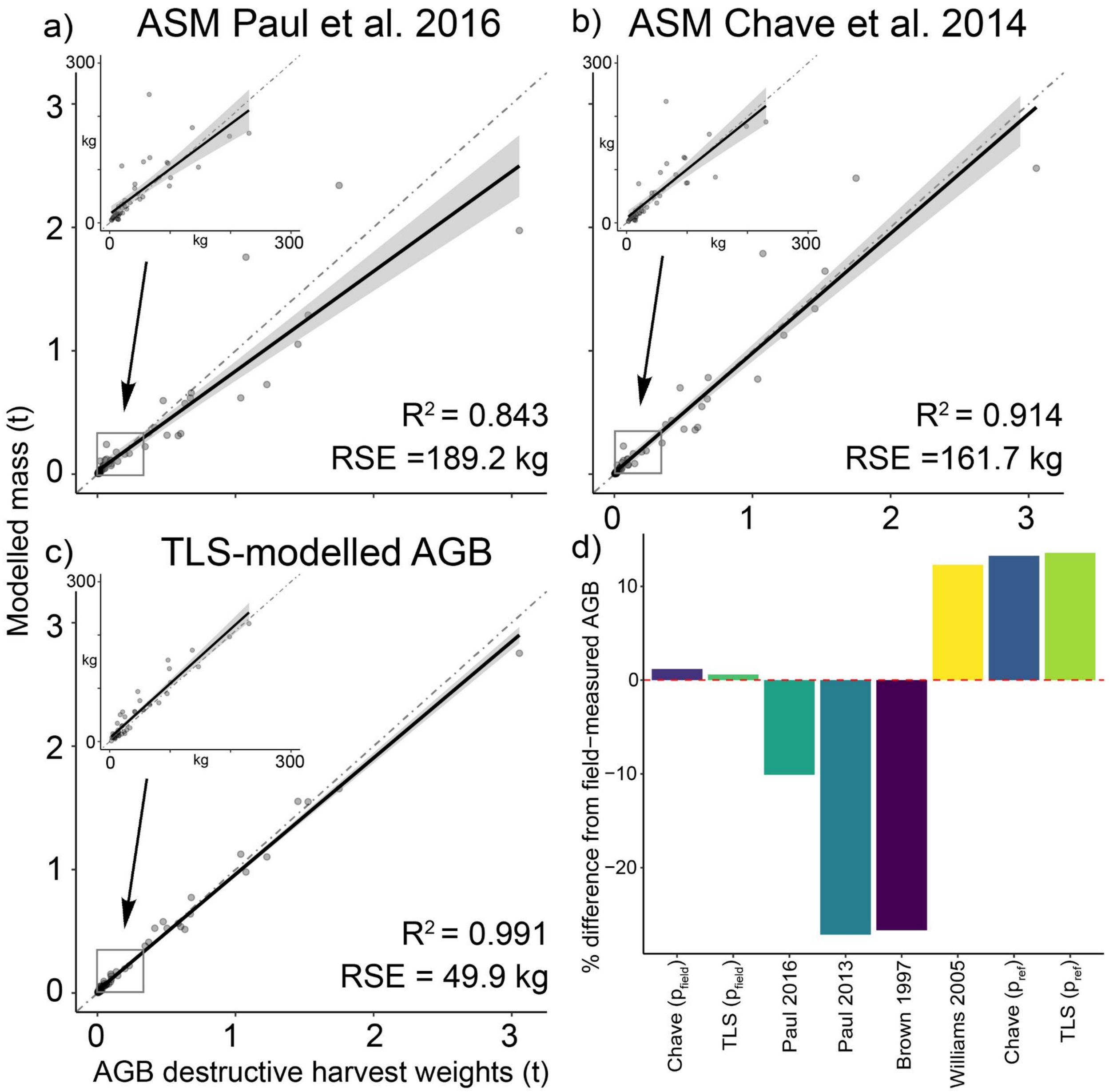

Figure 3 Observed AGB from destructive harvest plotted against modelled AGB using the two highest-performing ASMs (a: Paul (2016), b: Chave (2014)) and AGB estimates derived from TLS (c). Estimates from the Chave (2014) ASM (b) and TLS modelling (c), both use p_{field}. Grey shaded area represents a 95% confidence interval. Insets show trees <300 kg. Results for all models in Supplementary Fig. 1. d) Percentage deviation from field-measured AGB for all ASMs and TLS models. Red dashed line represents field-measured AGB (baseline for comparison).

Table 1 Model performance for tree AGB estimates from ASMs and TLS. Results for the Chave (2014) ASM and TLS modelling, which both apply p_{wood}, are shown here using values published in the Global Wood Density Database (Zanne, Amy E., 2009) (p_{ref}) as well as with field-measured species mean p_{field}.

Model	p_{wood} (g cm^{-3})	R^2	Slope	Intercept	RSE (kg)
Williams 2005	n/a	0.841	1.04	23.1	246.0
Paul 2016	n/a	0.843	0.81	26.4	189.2
Paul 2013	n/a	0.844	0.63	28.1	147.6
Brown 1997	n/a	0.842	0.65	24.4	152.8
Chave 2014	Reference	0.954	1.13	1.9	133.7
Chave 2014	Field	0.914	0.97	12.6	161.7
TLS	Reference	0.974	1.11	6.5	98.8
TLS	Field	0.991	0.94	18.4	49.9

Patterns of internal stem damage by species and position

Of 63 trees that were destructively harvested and modelled as QSMs, 32 trees (50.8%) had internal stem damage occurring in at least one cross-sectional sample. On average, damaged trees had 5% internal stem damage (SD = 6.65%), with as much as 30% damaged in some trees while the majority of trees carried 1-10% damage (94% of damaged trees, 48% of all trees). *Eucalyptus tetrodonta* trees were most frequently damaged (100%, n = 4) while *C. clarksoniana* trees had the greatest extent of internal stem damage (mean = 7.6%, SD = 8.6%, Supplementary Table 6). In our mixed effect model with individual tree (variance = 0.55, SD = 0.74) as a random effect, internal stem damage significantly decreased with increasing height in damaged trees (Fig. 4, beta = -0.02, 95% CI [-0.03, -0.02], t(154) = -9.48, conditional $R^2 = 0.61$, marginal $R^2 = 0.24$, $p < 0.001$). Internal damage was greatest and most frequent between the base of the tree and the first branching point (Fig. 4, Supplementary Table 4).

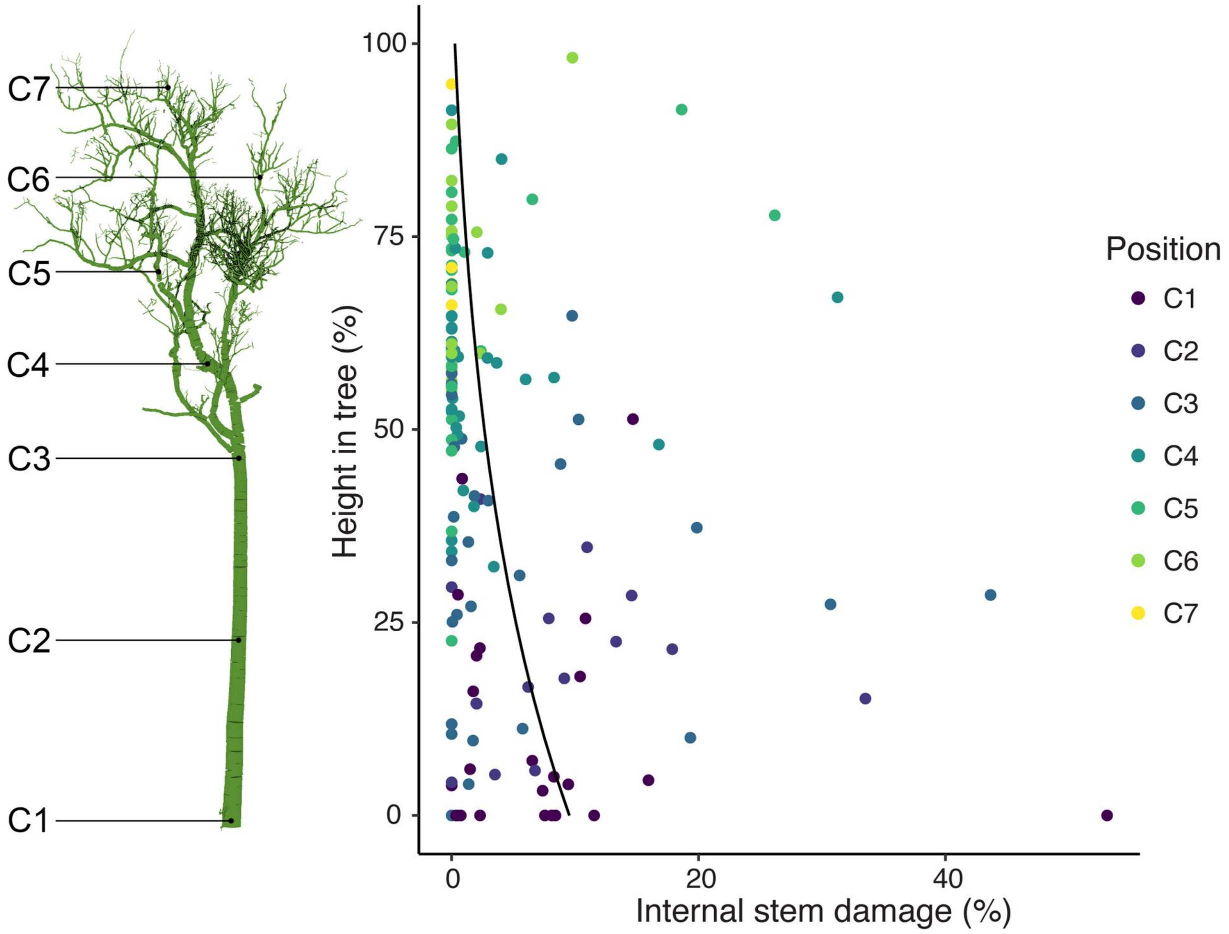

Figure 4 a) Relationship between height in tree (y-axis) and cross-sectional damage (x-axis, expressed as %) for all damaged trees in the study. Damage and variance are greatest toward the tree base, and less damage occurs with increasing height toward the canopy. Dots are colored by the position in which cross sections were taken from the tree.

Impact of internal stem damage and tree size on AGB estimates from TLS and ASMs

We found that percentage internal stem damage (beta = -0.039, p = 0.027) and tree DBH (beta = -0.014 , p = 0.00047) were significant predictors of TLS residuals, and there was a weak but significant interaction between tree DBH and percentage internal stem damage (beta = 0.0012, p = 0.04, Fig. 5a). TLS-estimated AGB of four large damaged trees was overestimated; however, AGB of large undamaged trees was accurately estimated. Small damaged trees were underestimated while small, undamaged trees were overestimated (Supplementary Fig. 6). Greater tree DBH and internal stem damage did not predict AGB overestimation using ASMs, and none of the five tested ASMs had a significant interaction between tree DBH and percentage internal stem damage (Fig. 5b).

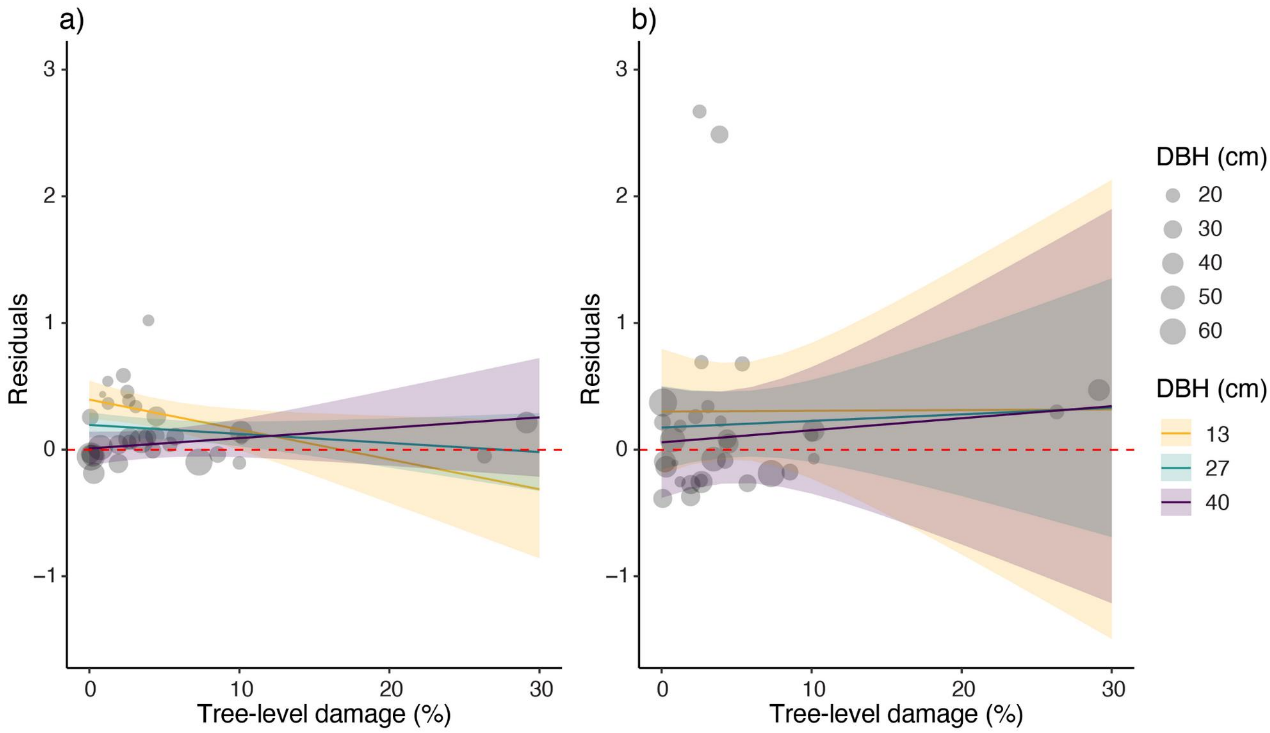

Figure 5 a) Predicted relationship (from linear model) between increasing internal damage (%) and TLS residuals (TLS-estimated AGB minus field-measured biomass, divided by tree size) for damaged trees. b) Predicted relationship (from linear model) between increasing internal damage and ASM residuals from Chave et al. (2014) (ASM-estimated AGB minus field-measured biomass, divided by tree size, applying p_{field}) for damaged trees. Points indicate residuals and % damage for individual trees (point size = DBH). Points above the red dashed line are overestimates of AGB, while points below are underestimates. Coloured lines show predicted relationships between internal damage and residuals for three DBH size classes.

Discussion

In the tropical savanna ecosystem studied here, TLS more accurately quantified AGB compared to multiple ASMs tested. TLS best captured plot-level AGB estimates, even with low levels (<10%) of internal stem damage present. These results are concordant with a recent meta-analysis that found ASMs to be less precise and less accurate than TLS at predicting AGB (Demol et al., 2022) and provide further support for TLS application in high-accuracy forest AGB and C measurement.

Using TLS, we estimated the total AGB of all destructively-harvested trees (18.4 t) to be within 0.6% of the field-measured value, a total error of 108 kg. We found that internal damage was concentrated in the lower region of the tree stem. The AGB of large trees with high internal damage was more likely to be overestimated by TLS as we hypothesized, however, AGB predictions from ASMs were unaffected by increasing amounts of internal stem damage. Together these results suggest that TLS is a highly accurate tool for estimating AGB at the plot- and tree-level if levels of internal damage are low. However, in ecosystems with large trees and higher levels of internal stem damage, C overestimation is likely. We will further discuss our results in relation to the application of TLS and ASM in broader applied contexts.

Internal stem damage and tree size affected AGB estimation using TLS and ASMs

Internal damage was consistently more frequent and extensive in the lower portion of the main stem, and we observed that many trees in the study sustained fire damage to the lower trunk, which may create favorable conditions allowing for microbial and termite entry. Due to its typically larger size, the main stem of a tree has more biomass to lose compared to the fine branches of the tree crown (Calders et al., 2015), so internal damage to the main stem has greater potential to reduce C storage. A noticeable characteristic of internal termite damage was carton nest material that filled in some hollow regions, which we were unable to fully remove in our field measurements of whole tree weights. Termite carton nest is likely less dense than the wood it replaced (R. Clement (personal communication, 2023)), yet this remains a limitation in detecting the true amount of AGB that termite hollowing removed.

We expected that tree-level AGB overestimations using TLS would result from high internal stem damage and over-modelling of small trees. In line with our expectations, we found that for larger trees, error in TLS-predicted AGB was explained by increasing levels of internal damage (Fig. 5a). In our study there were only 2 trees with >20% damage (Fig. 5b), and the majority of the damaged trees that we sampled had <10% internal stem damage with an average of 5%. Although greater internal stem damage increased TLS error, estimation of AGB at the plot-level was not significantly affected (Fig. 3d). Since large trees store a disproportionate amount of C in forests (Slik et al., 2013), capturing internal stem damage in large trees is an important consideration when TLS is used to estimate AGB for accuracy in forest C measurement.

AGB of small trees with low (<10%) damage tended to be overestimated by TLS (Fig. 5a), which is congruent with the findings for small trees from Demol et al. (2022) and is a documented artifact of TLS, which poorly captures very fine branches (Demol et al., 2022; Hackenberg et al., 2015; Wilkes et al., 2021). To correct for this problem, future work should fine-tune point clouds to avoid errors that inflate small tree models. For example, centroids of beams with multiple returns from small-diameter branches can be subjected to a calibrating adjustment to more accurately fit branches after initial modelling (Wilkes et al., 2021). However, although small tree AGB was less accurately predicted by TLS, the error did not adversely affect plot-level AGB estimates as small trees (<300 kg) represented only 11% of all AGB on the study plot.

Despite providing less accurate AGB estimations in comparison to TLS, the error associated with the ASMs tested here was not impacted by internal stem damage (Fig. 5b). This seemingly surprising finding can be attributed to the fact that the destructive harvest data underlying ASMs would have included internally damaged trees. However, the amount of such damage in these trees would not have been quantified, meaning that the generalizability and application to ecosystems with different levels of internal stem damage remains unclear. Unless an ASM is generated specifically to address internal stem damage (e.g. Monda et al. (2015)), the influence of damage on AGB estimation remains unquantified for ASMs. It is expected that ASMs generated for low damage systems should overestimate biomass in high damage systems (35% in dry savannas (Flores-Moreno et al., 2023); Monda et al. 2015, 42% in peat swamps (Monda et al., 2015)) without calibration.

Another source of error that could affect measures of AGB, which was not the main focus of this study, is biomass of foliage. Although the ASMs included here explicitly incorporate foliage, TLS-derived volume models do not. Due to time and logistical constraints we did not separately quantify the proportional biomass of foliage for all trees in this study; however, for four smaller trees (DBH range = 6.3-24.5 cm), we removed and measured canopy leaf mass. From this small subsample (assuming a leaf relative water content of 78%, (Schmidt et al., 1999)), leaf mass was estimated to be 1 to 4.9% of total AGB, with smaller trees having the highest foliage proportions. Other studies similarly reported foliage proportion of total AGB between 3 and 5% for eucalypt ecosystems (Kuyah et al., 2013; Werner & Murphy, 2001). Further, the ratio between leaf and total AGB in savanna ecosystems decreases with increasing tree size (Delitti et al., 2006). We estimate that if 4% biomass were added to TLS-based total AGB estimates to account for foliage, the plot-level error of this modelling approach would remain under +5% of destructive harvest tree weights.

Effect of wood specific gravity values on AGB estimates

We found that using field-measured wood specific gravities resulted in AGB estimates closer to field-measured values. For trees in our study, p_{ref} values were generally higher than p_{field} values (Supplementary Fig. 2), producing AGB overestimates from both TLS and ASMs. Measures of p_{field} better represented trees as they were site specific, whereas wood density databases compile values from across the globe and are therefore less representative of any given site. Database values also target a single point of undamaged heartwood toward the base of the tree, where it is most dense (Wassenberg et al., 2015). Measuring wood density at one point on the tree may fail to incorporate changing ratios of heartwood to sapwood with different stem sizes (Sellin, 1994). Interestingly, the Chave (2014) ASM had lower error when p_{ref} was used (Supplementary Table 7). This may be due to differences in p_{wood} for *L. suaveolens*, among the largest trees in the study (which strongly influence plot-level AGB, (Slik et al., 2013)), as this species and *P. nonda* were unusual in having higher p_{field} than p_{ref} (Supplementary Fig. 2). Taken together, for TLS-based AGB modelling, we conclude that the best estimates (in terms of R^2 and RSE) are derived from using p_{field}; however, p_{ref} still generated TLS-derived AGB estimates with a useful level of accuracy, as sampling trees to obtain p_{field} values is not always feasible.

Applications of TLS and ASMs for estimating AGB in a low-damage ecosystem

TLS provides the most accurate estimate of AGB for both aggregated plot-level biomass and individual tree estimates. The model developed by Chave et al. (2014), which incorporated an environmental stress variable (E) and p_{wood} as well as DBH, demonstrated the highest predictive power for ASMs. It is worth noting that the Chave (2014) ASM was developed using a >4,000-tree dataset that contained only a small portion of Australian trees, which contrasts with the Paul (2016) ASM of >15,000 Australian trees, which was tailored to represent Australian ecosystems, including savannas, and performed more poorly. This underscores how ASMs can be variable in predicting AGB (Fig. 3d, Table 1). TLS and ASMs may both estimate plot-level AGB with high accuracy, but application of each method depends on project goals and resources (Table 2). The considerably lower RSE of TLS AGB estimates is important for accurate monitoring and tracking tree growth changes over time in forests and woodlands (Sheppard et al., 2016). For situations in which estimating aggregated AGB is the primary goal, and where high levels of precision and accuracy are less important, ASMs are a functional option. However, given the high frequency of disturbance (i.e., cyclones and fires) in tropical regions which can cause considerable damage to standing AGB (Zuleta et al., 2023), the inability of ASMs to capture variation in tree crown morphology (e.g., snapped or burned trees) remains a limitation that TLS can overcome. As governments attempt to stem the tide of ecosystem destruction and rising CO_2 emissions with emerging environmental management strategies such as carbon and biodiversity markets (CCFI Act, 2011; NRMA 2023, 2023), the development of accurate, scalable tools for monitoring carbon in terrestrial ecosystems has become an urgent necessity.

To broaden the scope of high-accuracy AGB estimation, TLS can also be integrated into landscape-scale airborne laser scanning (ALS) point clouds, and these LiDAR-based approaches can be used to train machine learning models to interpret patterns related to vegetation structure in satellite imagery (Francis & Law, 2022; Liao et al., 2020). ASMs, in addition to being less accurate, are also difficult to integrate with landscape-scale remote sensing approaches such as

ALS. By providing detailed measurements of tree architecture, ecosystem structure, canopy cover, and other ecologically important structural attributes in a compatible spatial data format, TLS can translate accurate forest metrics to larger geographical scales with higher accuracy than ASMs. The deployment of LiDAR presents a new phase in forest science, with opportunities to deepen our understanding of global forest ecosystems and integrate these insights into effective carbon and biodiversity markets.

Table 2 Relative advantages and disadvantages of using TLS and ASMs to estimate AGB.

	TLS	**ASM**
Advantages	• Accuracy is very high • Fewer field personnel required • Measurements of canopy structure and branching are precise and repeatable • Stems and canopy are geolocated • Aerial LiDAR can be integrated	• Accessible measurement technology (DBH tape, clinometer) • Some regional and species-level allometries available
Disadvantages	• Initial outlay is higher • Species ID still requires field surveys • Small tree overestimation requires calibration • Currently more sensitive to internal stem damage	• Lower accuracy • In larger plots with high stem density, more field personnel required • Tree structural variation not captured • Destructive harvests required to build models • Integrates poorly with remote sensing data

Carbon estimation methods and internal stem damage in the context of carbon markets

Inaccurate estimations of tree AGB, whether due to measurement techniques (via either TLS or ASMs) or unmeasured biological factors such as internal stem damage, bring a risk of improperly valuing forest C and issuing carbon credits that fail to reflect reality. The average size of a carbon estimation area (CEA) in the Australian carbon market is 18,981 ha (mean size of 223 Human-Induced Regeneration CEAs, (*Clean Energy Regulator*, 2023)). At the rates of C per hectare observed in this study (63.36 t), using the highest-performing ASM by Chave et al. (2014) on a project of this size would result in an overvaluation of 16,538 Australian carbon credit units (ACCUs, correspond to 1 tonne CO_2) (worth $317,378 USD). Using TLS, 8,340 ACCUs would be incorrectly over credited, representing a value of $160,045 (ACCU price July 2023, www.accus.com.au). In theory, if ASMs for other vegetation types were as inaccurate as this pantropical model, using TLS for carbon estimation from AGB could reduce over-allocation of ACCUs by 50%.

While the low levels of internal stem damage at our study site did not significantly alter overall AGB estimates, higher levels of internal stem damage could pose more serious consequences for accuracy of forest carbon measurement. Future work is needed to disentangle tree traits that predict susceptibility to damage, the consequences of how termite and microbial decomposition affects carbon storage, and how fire may promote or interact with internal damage. Less invasive tools such as resistograph drills or sonic tomography can be used to estimate damage in the main stem (Flores-Moreno et al., 2023; Gilbert et al., 2016), where we have shown it is most acute. Quantifying internal stem damage in this way can determine if it is a significant source of error that should be considered in a forest carbon project.

Supporting information

Supplementary Table 1 Sampling of tree cross-sections used in assessing internal stem damage.

Cross-section	Description
C1	Scarf cut point - tree felled here (~1m from the ground)
C2	Cut point between C1 and C3, sampled for trees with damage at C1 and C3
C3	Cut point 50 cm below first branching point
C4	Cut point at branch order 2 - canopy branches (mean = 14.7 cm, SD = 9.2)
C5	Cut point at branch order 3 - canopy branches (mean = 8.9 cm, SD = 4.8)
C6	Cut point at branch order 4 - canopy branches (mean = 6.5 cm, SD = 2.0)
C7	Cut point at branch order 5 - canopy branches (mean = 5.7cm, SD = 2.3)

Supplementary Table 2 Reference wood specific gravities (Global Wood Density Database, Zanne et al. 2009) of closest available relatives from published sources for species in this study that did not have available published wood specific gravity values. Wood specific gravity is in g cm-3.

Species	Reference species	Reference specific gravity	Phylogeny reference
Acacia polystachya	*A. acuminata*	1.008	Murphy et al. 2010
Corymbia clarksoniana	*C. gummifera*	0.869	Parra et al. 2006
Grevillea parallela	*G. wickhamii*	0.680	Mast et al. 2015
Planchonia careya	*P. papuana*	0.645	Prance et al. 2013

Supplementary Table 3 Allometric scaling models (ASMs) that were compared with TLS-based AGB estimates. DBH in ASM equations is in cm. Plant functional types from Paul et al. (2016) are: single-stemmed eucalypt (**F_{Euc}**); single-stemmed non-eucalypt, high wood specific gravity (**$F_{Other\text{-}H}$**); single-stemmed non-eucalypt, low wood specific gravity (**$F_{Other\text{-}L}$**). Wood specific gravity is in g cm^{-3}.

Author	**Regression dataset**	**Equations**
Williams et al. (2005)	220 trees: 14 woodland tree spp., mainly eucalypts (Australia)	**5a** =EXP(-2.2111 + 2.4831 * LN(*DBH*))
Paul et al. (2016)	15,054 trees: 5 broad categories of plant functional type (Australia)	**F_{Euc}** =EXP(2.016 + 2.375 * LN(*DBH*) * 1.067) **$F_{Other\text{-}H}$** =EXP(1.693 + 2.220 * LN(*DBH*) * 1.044) **$F_{Other\text{-}L}$** =EXP(2.573 + 2.460 * LN(*DBH*) * 1.018)
Paul et al. (2013)	3,139 trees: mixed tree and shrub communities (Australia)	**Universal tree <100 cm** =EXP(-1.82 + 2.27 * LN(*DBH*))
Brown (1997)	5,300 trees: tropical dry forest spp. (India) Revised from *Brown et al. (1989)*	**Equation 3.2.1** =EXP(-1.996 + 2.32 * LN(*DBH*))
Chave et al. (2014)	4,004 trees: range of tropical spp. (Globally distributed)	**Equation 7** =EXP(-1.803 - 0.976 * *E* + 0.976 * LN(*wood specific gravity*) + 2.673 * LN(*DBH*) - 0.0299 * (LN(*DBH*)^2))

Supplementary Table 4 For damaged trees, damage frequency (%), average damage (%), and standard deviation of damage for cross sectional samples at different sampled positions across tree height.

Position	**n**	**Damage frequency (%)**	**Average cross section damage (%)**	**SD**
C1	36	97.2	9.97	12.22
C2	15	86.7	8.67	8.78
C3	31	67.7	5.39	10.13
C4	33	57.6	2.64	6.13
C5	31	22.6	1.78	5.73
C6	17	23.5	1.07	2.52
C7	4	0.0	0.0	0

Supplementary Table 5 For damaged trees, linear regression model parameters describing relationship between internal stem damage and vertical position in the tree.

Tree	Tree ID	Species	Intercept	Slope	R^2	p
1	Extra2_lower	*Lophostemon suaveolens*	0.1157	-0.0041	0.0739	0.72820
2	9_lower	*Corymbia clarksoniana*	-21.5981	3.0176	0.9991	0.00045
3	10_lower	*Corymbia clarksoniana*	-2.4442	0.3514	0.4803	0.51254
4	11_lower	*Corymbia clarksoniana*	-2.6978	0.4286	0.4707	0.13235
5	15_lower	*Eucalyptus tetrodonta*	-2.1015	0.2086	0.4387	0.15177
6	2_lower	*Corymbia clarksoniana*	-2.5217	0.2238	0.5610	0.05268
7	Cor1_lower	*Corymbia clarksoniana*	-16.6277	2.2180	0.9042	0.04911
8	12_lower	*Corymbia clarksoniana*	-10.9190	1.0447	0.5718	0.13912
9	4_lower	*Corymbia clarksoniana*	-5.1996	0.4938	0.5272	0.10225
10	19_lower	*Corymbia clarksoniana*	-7.2390	0.7081	0.8052	0.01527
11	16_lower	*Eucalyptus tetrodonta*	8.6170	-0.0403	0.0110	0.84297
12	6_lower	*Corymbia tessellaris*	-0.3202	0.0367	0.7152	0.03389
13	8_lower	*Corymbia clarksoniana*	-0.1454	0.0131	0.2987	0.34050
14	Test	*Corymbia clarksoniana*	-5.2317	0.8955	0.4852	0.19125
15	17_lower	*Corymbia clarksoniana*	2.1073	1.9591	0.3968	0.25474
16	Extra7_lower	*Corymbia clarksoniana*	-6.5768	0.8492	0.7656	0.02246
17	18_lower	*Eucalyptus tetrodonta*	-0.1886	0.1385	0.7151	0.07110
18	Extra3_lower	*Planchonia careya*	-3.6337	0.5868	0.7802	0.31064
19	13_lower	*Lophostemon suaveolens*	0.4271	0.0770	0.2135	0.53796
20	3_lower	*Eucalyptus tetrodonta*	-6.7954	0.5414	0.7593	0.02375
21	Planch1_lower	*Planchonia careya*	-11.6701	1.4462	0.9041	0.04915
22	Planch2_lower	*Planchonia careya*	-1.6325	0.3172	0.5903	0.12914
23	Loph1_lower	*Lophostemon suaveolens*	-3.4348	0.5498	0.9148	0.18852
24	1_lower	*Lophostemon suaveolens*	-0.0939	0.0049	0.7354	0.06313
25	5_lower	*Planchonia careya*	0.2668	0.0938	0.0792	0.71865
26	Cor1_upper	*Corymbia clarksoniana*	-0.0195	0.8387	0.2984	0.45376
27	Golden1_upper	*Deplanchea tetraphylla*	-4.2921	0.6621	0.6978	0.37056
28	Loph2_upper	*Lophostemon suaveolens*	-3.3602	0.7108	0.3361	0.42024
29	6_upper	*Corymbia clarksoniana*	-0.6254	0.1454	0.2201	0.34796

30	3_upper	*Lophostemon suaveolens*	-0.1010	0.0147	0.4259	0.16004
31	4_upper	*Corymbia clarksoniana*	-5.4423	1.3801	0.8820	0.00545
32	5_upper	*Parinari nonda*	0.1536	0.0073	0.0579	0.69650

Supplementary Table 6 Internal damage frequency (percentage of trees in study) and extent (mean percentage of total tree AGB and standard deviation).

Species	n	Damage frequency (%)	Damage mean (%)	Damage SD
Eucalyptus tetrodonta	4	100	4.4	2.0
Corymbia clarksoniana	16	94	7.6	8.6
Lophostemon suaveolens	11	55	1.0	1.9
Parinari nonda	2	50	0.1	0.2
Deplanchea tetraphylla	3	33	0.8	1.5
Planchonia careya	20	20	0.4	0.9

Supplementary Table 7 TLS and Chave 2014 ASM model performance using reference and field-measured wood specific gravity.

Model	**p_{wood}**	**R^2**	**Slope**	**Intercept**	**RSE (kg)**
Chave 2014	reference	0.9543	1.13	2.43	133.8
	field-measured	0.9136	0.97	13.05	161.8
TLS	reference	0.9740	1.11	6.49	98.8
	field-measured	0.9908	0.94	18.38	49.9

Supplementary Table 8 Sum of observed dry tree weights, net difference from field-measured biomass (kg), and percentage difference from field-measured biomass. The ASM of Chave et al. (2014) and TLS model use p_{field}.

	Total weight (kg)	**Difference from field-measured biomass (kg)**	**Difference from field-measured biomass (%)**
Observed dry ABG	18,438	0.00	0.00
Williams 2005 ASM	20,705	2,266	+12.30
Paul 2016 ASM	16,578	-1,860	-10.10
Paul 2013 ASM	13,435	-5,003	-27.10
Brown 1997 ASM	13,524	-4,914	-26.70
Chave 2014 ASM (p_{field})	18,654	216	+1.20
Chave 2014 ASM (p_{ref})	20,881	2,443	+13.20
TLS (p_{field})	18,546	108	+0.59
TLS (database p_{ref})	20,940	2,502	+13.60

Supplementary Table 9 Number of individuals for each species in the study

Species	n
Acacia polystachya	1
Corymbia clarksoniana	16
Corymbia tessellaris	2
Deplanchea tetraphylla	3
Eucalyptus tetrodonta	4
Grevillea parallela	3
Lophostemon suaveolens	11
Parinari nonda	2
Planchonia careya	20
Timonius timon	1

Supplementary Table 10 Output for wood density linear mixed model model for undamaged cross sections. Wood specific gravity is predicted by cross section diameter (in cm) and species, and tree ID is included as a random effect.

Fixed effects	Estimate	SE	t-value	p-value
Intercept	8.136e-05	3.979e-02	20.445	< 0.001
diameter_cm	5.861e-05	7.707e-04	0.076	0.939
speciesCorymbia clarksoniana	-2.133e-01	3.881e-02	-5.496	< 0.001
speciesCorymbia tessellaris	-1.363e-01	5.625e-02	-2.423	< 0.001
speciesDeplanchea tetraphylla	-3.887e-01	5.664e-02	-6.862	< 0.001
speciesEucalyptus tetrodonta	-1.836e-01	4.409e-02	-4.164	< 0.001
speciesGrevillea parallela	-1.821e-01	5.696e-02	-3.197	0.002
speciesLophostemon suaveolens	-2.650e-01	3.873e-02	-6.842	< 0.001
speciesParinari nonda	-2.826e-01	5.245e-02	-5.387	< 0.001
speciesPlanchonia careya	-3.260e-01	4.025e-02	-8.098	< 0.001

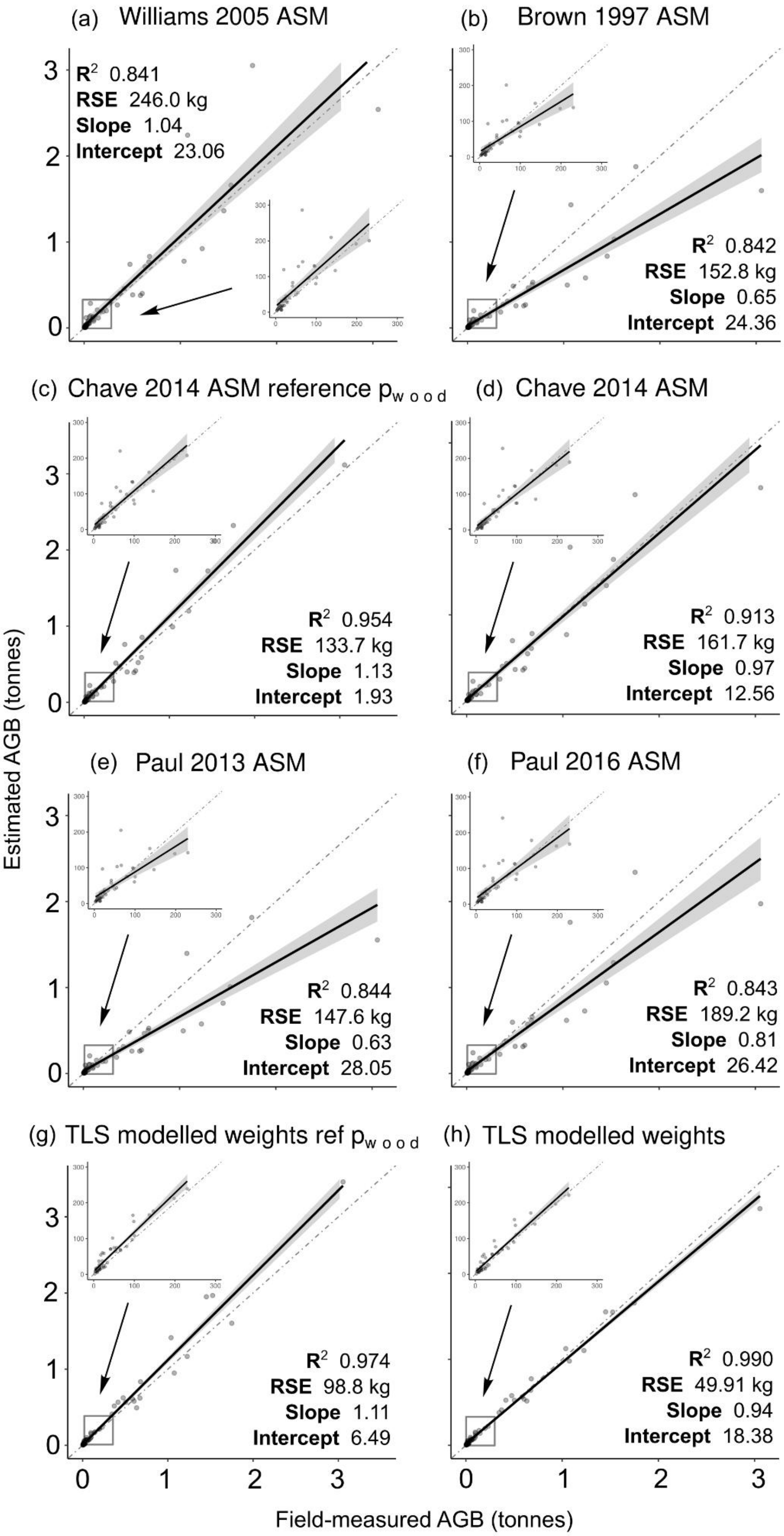

Supplementary Figure 1 Estimated and observed AGB for all ASM models tested in this study (a-f) and TLS (g,h). Results for the ASM published by Chave et al. (2014) are presented using both published (c) and field-measured (d) wood specific gravities. Results for TLS are also presented using published (g) and field (h) wood specific gravities. Results for smaller trees (0-300 kg) are also shown in inset plots.

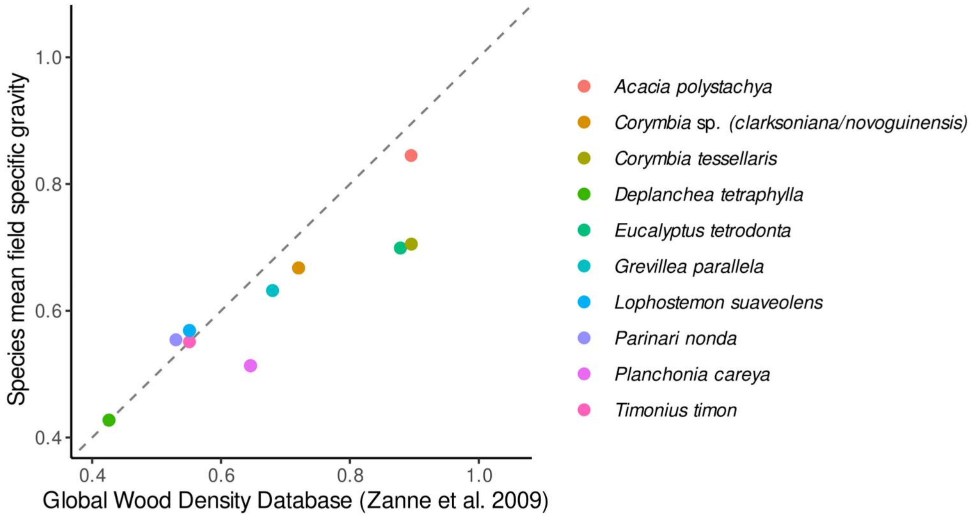

Supplementary Figure 2 Comparison of species mean wood specific gravities collected in this study with generalized species densities published in the Global Wood Density Database (Zanne et al. 2009).

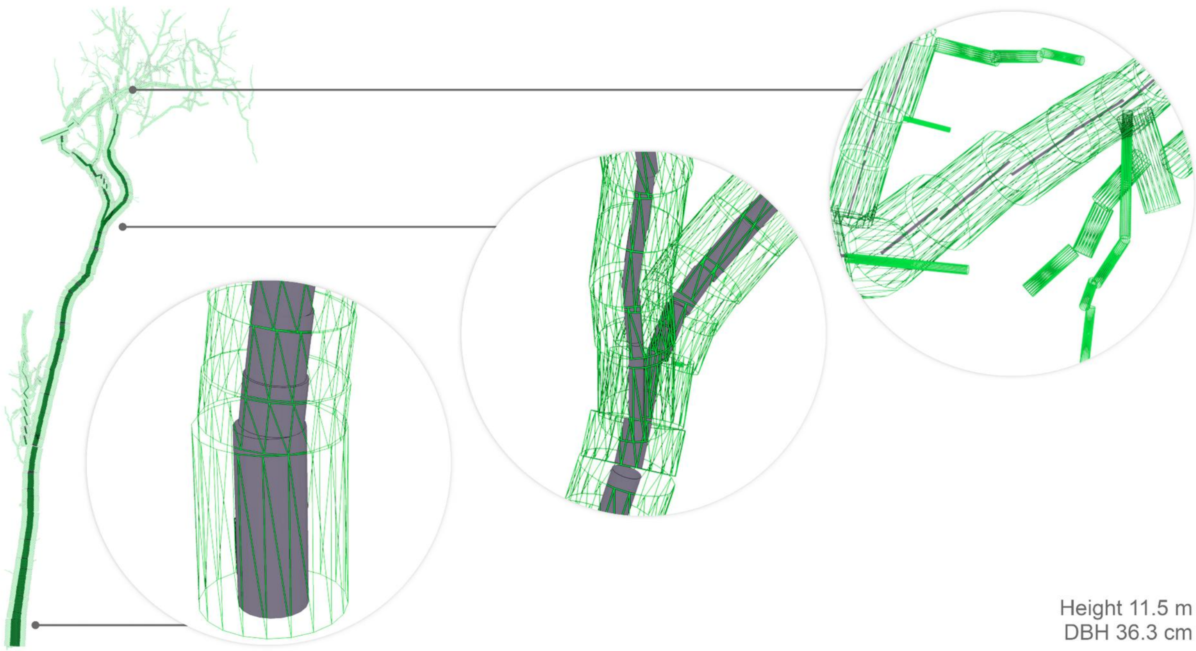

Supplementary Figure 3 Quantitative structural model (QSM) of *Corymbia clarksoniana* (green) with internal damage modelled from linear regression (grey) for all cylinders in the model. This was the most internally damaged tree in the dataset (see Fig. 2).

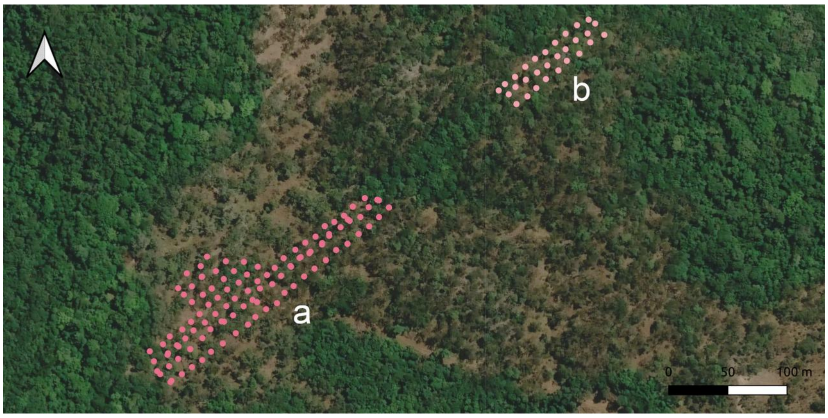

Supplementary Figure 4 Scan plot layouts of Plots A and B. Each point represents a position from which a single scan was taken.

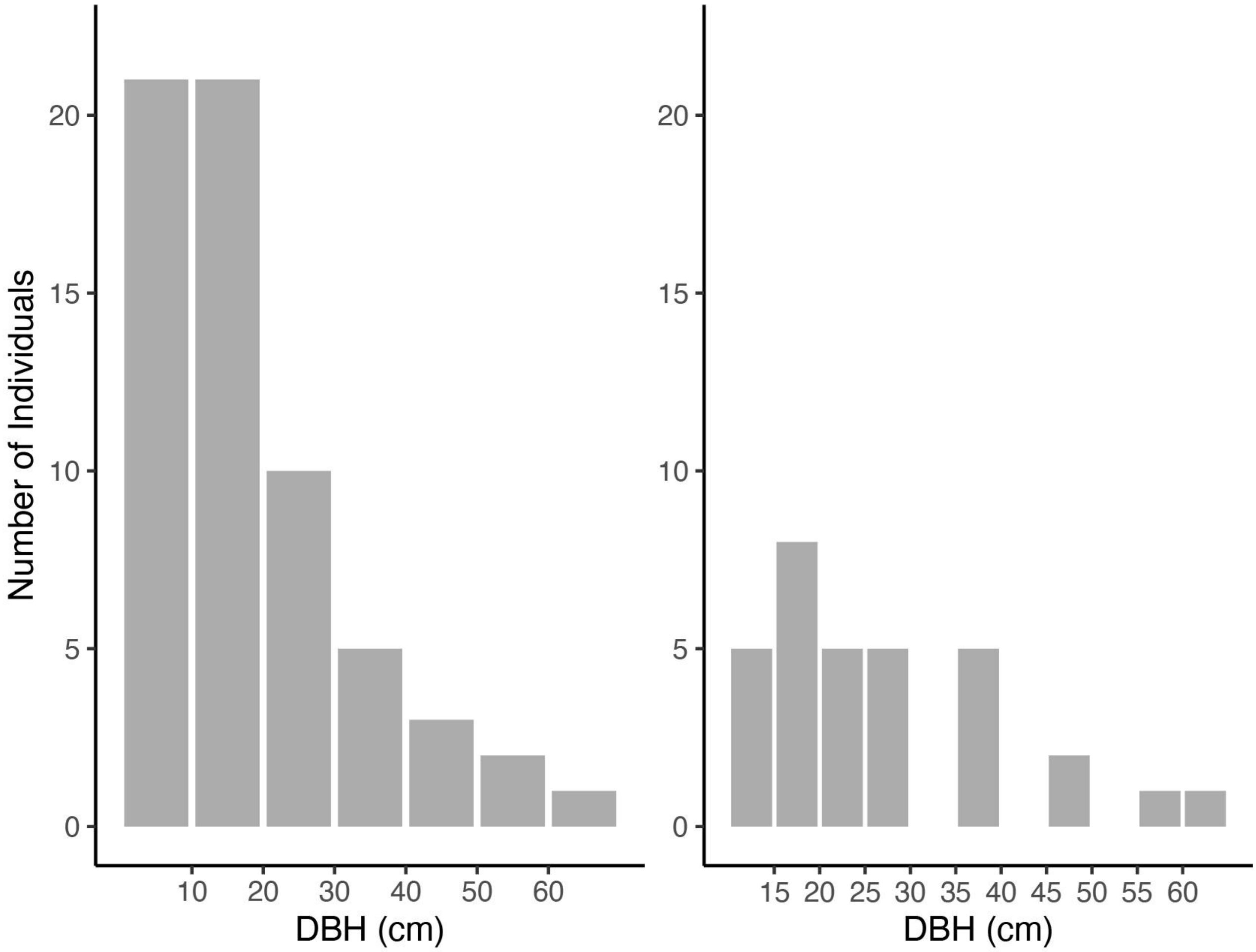

Supplementary Figure 5 a) DBH size distribution (cm) of all trees (n = 63) in the study and b) DBH size distribution (cm) of damaged trees in study (n = 32).

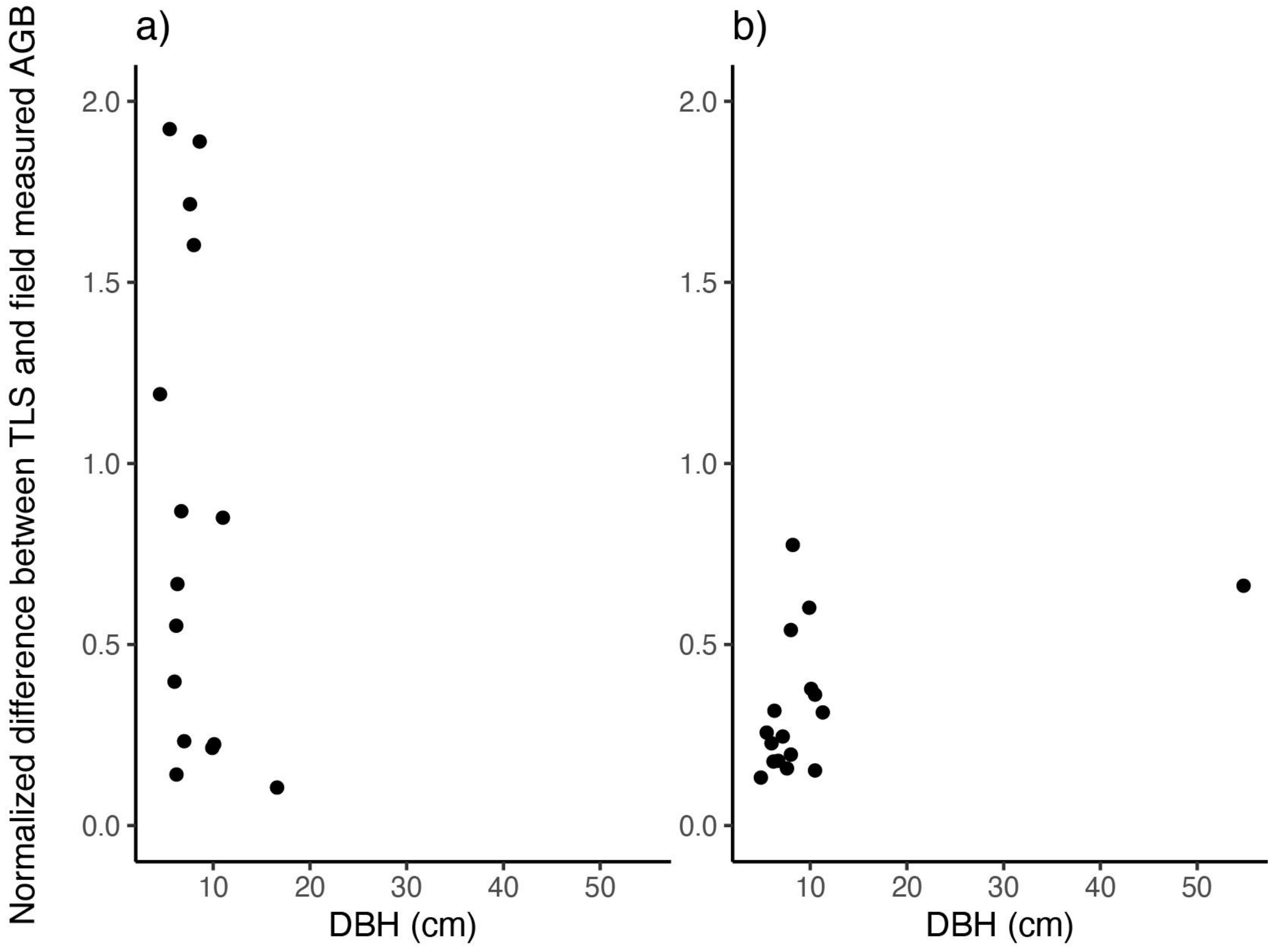

Supplementary Figure 6 Distribution of over/underestimates of field-measured biomass from TLS (a) and Chave 2014 ASM (b) for undamaged trees, normalized by tree size. Values over y = 0 correspond to an overestimate of biomass, while those less than y = 0 indicate an AGB underestimation.

Supplementary Data 1 Segmented point cloud files (.PCD) and cylinder models (.PLY) for all destructively harvested trees; Python script used to cut QSMs at scarf for trees felled above ground level (link Zenodo).

References

Adkins, M. F. (2006). A burning issue: Using fire to accelerate tree hollow formation in *Eucalyptus* species. *Australian Forestry*, *69*(2), 107–113. https://doi.org/10.1080/00049158.2006.10676236

Apolinário, F. E., & Martius, C. (2004). Ecological role of termites (Insecta, Isoptera) in tree trunks in central Amazonian rain forests. *Forest Ecology and Management*, *194*(1–3), 23–28. https://doi.org/10.1016/j.foreco.2004.01.052

Australian Bureau of Meteorology. (2023). *Queensland Observations* [dataset]. http://www.bom.gov.au/qld/observations/index.shtml?ref=hdr

Baskerville, G. L. (1972). Use of Logarithmic Regression in the Estimation of Plant Biomass. *Canadian Journal of Forest Research*, *2*(1), 49–53. https://doi.org/10.1139/x72-009

Bastin, J.-F., Finegold, Y., Garcia, C., Mollicone, D., Rezende, M., Routh, D., Zohner, C. M., & Crowther, T. W. (2019). The global tree restoration potential. *Science*, *365*(6448), 76–79. https://doi.org/10.1126/science.aax0848

Beck, H. E., Zimmermann, N. E., McVicar, T. R., Vergopolan, N., Berg, A., & Wood, E. F. (2018). Present and future Köppen-Geiger climate classification maps at 1-km resolution. *Scientific Data*, *5*(1), 180214. https://doi.org/10.1038/sdata.2018.214

Brown, I. F., Martinelli, L. A., Thomas, W. W., Moreira, M. Z., Cid Ferreira, C. A., & Victoria, R. A. (1995). Uncertainty in the biomass of Amazonian forests: An example from Rondônia, Brazil. *Forest Ecology and Management*, *75*(1–3), 175–189. https://doi.org/10.1016/0378-1127(94)03512-U

Brown, S. (1997). *Estimating Biomass and Biomass Change of Tropical Forests: A Primer*. Food & Agriculture Org.

Burt, A., Boni Vicari, M., Da Costa, A. C. L., Coughlin, I., Meir, P., Rowland, L., & Disney, M. (2021). New insights into large tropical tree mass and structure from direct harvest and terrestrial lidar. *Royal Society Open Science*, *8*(2). https://doi.org/10.1098/rsos.201458

Burt, A., Disney, M., & Calders, K. (2019). Extracting individual trees from lidar point clouds using treeseg. *Methods in Ecology and Evolution*, *10*(3), 438–445. https://doi.org/10.1111/2041-210X.13121

Calders, K., Newnham, G., Burt, A., Murphy, S., Raumonen, P., Herold, M., Culvenor, D., Avitabile, V., Disney, M., Armston, J., & Kaasalainen, M. (2015). Nondestructive estimates of above-ground biomass using terrestrial laser scanning. *Methods in Ecology and Evolution*, *6*(2), 198–208. https://doi.org/10.1111/2041-210X.12301

Carbon Credits (Carbon Farming Initiative) Act 2011, (2011). https://www.legislation.gov.au/Details/C2011A00101

Chave, J., Andalo, C., Brown, S., Cairns, M. A., Chambers, J. Q., Eamus, D., Fölster, H., Fromard, F., Higuchi, N., Kira, T., Lescure, J.-P., Nelson, B. W., Ogawa, H., Puig, H., Riéra, B., & Yamakura, T. (2005). Tree allometry and improved estimation of carbon stocks and balance in tropical forests. *Oecologia*, *145*(1), 87–99. https://doi.org/10.1007/s00442-005-0100-x

Chave, J., Réjou-Méchain, M., Búrquez, A., Chidumayo, E., Colgan, M. S., Delitti, W. B. C., Duque, A., Eid, T., Fearnside, P. M., Goodman, R. C., Henry, M., Martínez-Yrízar, A., Mugasha, W. A., Muller-Landau, H. C., Mencuccini, M., Nelson, B. W., Ngomanda, A., Nogueira, E. M., Ortiz-Malavassi, E., … Vieilledent, G. (2014). Improved allometric models to estimate the aboveground biomass of tropical trees. *Global Change Biology*, *20*(10), 3177–3190. https://doi.org/10.1111/gcb.12629

Clean Energy Regulator. (2023). https://www.cleanenergyregulator.gov.au/

Clement, R. (2023). *Termite carton nest is likely less dense than the wood it replaced* [Personal communication].

Delitti, W. B. C., Meguro, M., & Pausas, J. G. (2006). Biomass and mineralmass estimates in a" cerrado" ecosystem. *Brazilian Journal of Botany*, *29*, 531–540.

Demol, M., Verbeeck, H., Gielen, B., Armston, J., Burt, A., Disney, M., Duncanson, L., Hackenberg, J., Kükenbrink, D., Lau, A., Ploton, P., Sewdien, A., Stovall, A., Takoudjou, S. M., Volkova, L., Weston, C., Wortel, V., & Calders, K. (2022). Estimating forest above-ground biomass with terrestrial laser scanning: Current status and future directions. *Methods in Ecology and Evolution*, *13*(8), 1628–1639. https://doi.org/10.1111/2041-210X.13906

Eleuterio, A. A., de Jesus, M. A., & Putz, F. E. (2020). Stem decay in live trees: Heartwood hollows and termites in five timber species in eastern Amazonia. *Forests*, *11*(10), 1–12. https://doi.org/10.3390/f11101087

Eyre, T. J., Kelly, A. L., Neldner, V. J., Wilson, B. A., Ferguson, D. J., Laidlaw, M. J., & Franks, A. J. (2015). BioCondition: A condition assessment framework for terrestrial biodiversity in Queensland. Assessment manual, Version 2.2. *Information Technology, Innovation and Arts, Brisbane*.

Flores-Moreno, H., Yatsko, A. R., Cheeseman, A. W., Allison, S. D., Cernusak, L. A., Cheney, R., Clement, R., Cooper, W., Eggleton, P., Jensen, R., Rosenfield, M., & Zanne, A. E. (2023). *Higher internal stem damage in dry compared to wet tropics: Where are we overestimating forest biomass?* https://ecoevorxiv.org/repository/view/5668/

Francis, J., & Law, S. (2022). *Estimating Chicago's tree cover and canopy height using multi-spectral satellite imagery* (arXiv:2212.05061). arXiv. https://doi.org/10.48550/arXiv.2212.05061

Frith, C., & Frith, D. (1993). Notes on birds found nesting at Iron Range, Cape York Peninsula, November-December 1890. *SUNBIRD*, *23*(2), 44–58.

Gilbert, G. S., Ballesteros, J. O., Barrios-Rodriguez, C. A., Bonadies, E. F., Cedeño-Sánchez, M. L., Fossatti-Caballero, N. J., Trejos-Rodríguez, M. M., Pérez-Suñiga, J. M., Holub-Young, K. S., Henn, L. A. W., Thompson, J. B., García-López, C. G., Romo, A. C., Johnston, D. C., Barrick, P. P., Jordan, F. A., Hershcovich, S., Russo, N., Sánchez, J. D., … Hubbell, S. P. (2016). Use of sonic tomography to detect and quantify wood decay in living trees. *Applications in Plant Sciences*, *4*(12), 1600060–1600060. https://doi.org/10.3732/apps.1600060

Hackenberg, J., Spiecker, H., Calders, K., Disney, M., & Raumonen, P. (2015). SimpleTree—An efficient open source tool to build tree models from TLS clouds. *Forests*, *6*(11), 4245–4294. https://doi.org/10.3390/f6114245

Heineman, K. D., Russo, S. E., Baillie, I. C., Mamit, J. D., Chai, P. P. K., Chai, L., Hindley, E. W., Lau, B. T., Tan, S., & Ashton, P. S. (2015). Evaluation of stem rot in 339 Bornean tree species: Implications of size, taxonomy, and soil-related variation for aboveground biomass estimates. *Biogeosciences*, *12*(19), 5735–5751. https://doi.org/10.5194/bg-12-5735-2015

Henry, M., Bombelli, A., Trotta, C., Alessandrini, A., Birigazzi, L., Sola, G., Vieilledent, G., Santenoise, P., Longuetaud, F., Valentini, R., Picard, N., & Saint-André, L. (2013). GlobAllomeTree: International platform for tree allometric equations to support volume, biomass and carbon assessment. *iForest - Biogeosciences and Forestry*, *6*(6), 326. https://doi.org/10.3832/ifor0901-006

Hirata, Y., Takao, G., Sato, T., & Toriyama, J. (2012). *REDD-plus COOKBOOK*.

Janzen, D. H. (1976). Why Tropical Trees Have Rotten Cores. *Biotropica*, *8*(2), 110–110.

Ketterings, Q. M., Coe, R., Van Noordwijk, M., Ambagau', Y., & Palm, C. A. (2001). Reducing uncertainty in the use of allometric biomass equations for predicting above-ground tree biomass in mixed secondary forests. *Forest Ecology and Management*, *146*(1–3), 199–209. https://doi.org/10.1016/S0378-1127(00)00460-6

Köhl, M., Magnussen, S. S., & Marchetti, M. (2006). *Sampling Methods, Remote Sensing and GIS Multiresource Forest Inventory*. Springer Science & Business Media.

Kuyah, S., Dietz, J., Muthuri, C., van Noordwijk, M., & Neufeldt, H. (2013). Allometry and partitioning of above- and below-ground biomass in farmed eucalyptus species dominant in Western Kenyan agricultural landscapes. *Biomass and Bioenergy*, *55*, 276–284. https://doi.org/10.1016/j.biombioe.2013.02.011

Lemmens, M. (2011). Terrestrial Laser Scanning. In M. Lemmens (Ed.), *Geo-information: Technologies, Applications and the Environment* (pp. 101–121). Springer Netherlands. https://doi.org/10.1007/978-94-007-1667-4_6

Liao, Z., van Dijk, A., He, B., Larraondo, P., & Scarth, P. (2020). Woody vegetation cover, height and biomass at 25-m resolution across Australia derived from multiple site, airborne and satellite observations. *International Journal of Applied*

Earth Observation and Geoinformation, *93*, 102209. https://doi.org/10.1016/j.jag.2020.102209

Martin, A. R., Doraisami, M., & Thomas, S. C. (2018). Global patterns in wood carbon concentration across the world's trees and forests. *Nature Geoscience*, *11*(12), 915–920. https://doi.org/10.1038/s41561-018-0246-x

Mascaro, J., Litton, C., Hughes, R., Uowolo, A., & Schnitzer, S. (2011). Minimizing Bias in Biomass Allometry: Model Selection and Log-Transformation of Data. *Biotropica*, *43*, 649–653. https://doi.org/10.1111/j.1744-7429.2011.00798.x

Momo Takoudjou, S., Ploton, P., Sonké, B., Hackenberg, J., Griffon, S., de Coligny, F., Kamdem, N. G., Libalah, M., Mofack, G., Le Moguédec, G., Pélissier, R., & Barbier, N. (2018). Using terrestrial laser scanning data to estimate large tropical trees biomass and calibrate allometric models: A comparison with traditional destructive approach. *Methods in Ecology and Evolution*, *9*(4), 905–916. https://doi.org/10.1111/2041-210X.12933

Monda, Y., Kiyono, Y., Melling, L., Damian, C., & Chaddy, A. (2015). Allometric equations considering the influence of hollow trees: A case study for tropical peat swamp forest in Sarawak. *Tropics*, *24*(1), 11–22. https://doi.org/10.3759/tropics.24.11

Nature Repair Market Bill 2023, (2023). https://www.legislation.gov.au/Details/C2023B00056

N'Dri, A. B., Gignoux, J., Konaté, S., Dembélé, A., & Aïdara, D. (2011). Origin of trunk damage in West African savanna trees: The interaction of fire and termites. *Journal of Tropical Ecology*, *27*(3), 269–278. https://doi.org/10.1017/S026646741000074X

Neldner, V., Butler, D., Guymer, G., Fensham, R., Holman, J., Cogger, H., Ford, H., Johnson, C., Holman, J., Butler, D., & others. (2017). Queensland's Regional Ecosystems. Building and maintaining a biodiversity inventory, planning framework and information system for Queensland. *Information Technology and Innovation, PO Box*, *5078*.

Pan, Y., Richard, A., Pekka, E., Werner, A., Oliver, L., Simon, L., Josep, G., Robert, B., Stephen, W., & David, A. (2011). A large and persistent carbon sink in the world's forests. *Science*, *333*(August), 988–993.

Panshin, AJ, & De Zeeuw, C. (1980). *Textbook of wood technology. Part 1. Formation, anatomy, and properties of wood*.

Paul, K. I., Roxburgh, S. H., Chave, J., England, J. R., Zerihun, A., Specht, A., Lewis, T., Bennett, L. T., Baker, T. G., Adams, M. A., Huxtable, D., Montagu, K. D., Falster, D. S., Feller, M., Sochacki, S., Ritson, P., Bastin, G., Bartle, J., Wildy, D., … Sinclair, J. (2016). Testing the generality of above-ground biomass allometry across plant functional types at the continent scale. *Global Change Biology*, *22*(6), 2106–2124. https://doi.org/10.1111/gcb.13201

Paul, K. I., Roxburgh, S. H., England, J. R., Ritson, P., Hobbs, T., Brooksbank, K., John Raison, R., Larmour, J. S., Murphy, S., Norris, J., Neumann, C., Lewis, T., Jonson, J., Carter, J. L., McArthur, G., Barton, C., & Rose, B. (2013). Development and testing of allometric equations for estimating above-ground biomass of mixed-species environmental plantings. *Forest Ecology and Management*, *310*, 483–494. https://doi.org/10.1016/j.foreco.2013.08.054

Perry, D. H., Lenz, M., & Watson, J. A. L. (1985). Relationships between fire, fungal rots and termite damage in Australian forest trees. *Australian Forestry*, *48*(1), 46–53. https://doi.org/10.1080/00049158.1985.10674422

Pillsbury, N. H., & Kirkley, M. L. (1984). Equations for total, wood, and saw-log volume for thirteen California hardwoods. *Res. Note PNW-RN-414. Portland, OR: U.S. Department of Agriculture, Forest Service, Pacific Northwest Research Station. 52 p*, *414*. https://doi.org/10.2737/PNW-RN-414

Ploton, P., Barbier, N., Stéphane, M., Réjou-Méchain, M., Bosela, F., Chuyong, G., Dauby, G., Droissart, V., Fayolle, A., Goodman, R., Henry, M., Kamdem, N., Mukirania, J., Kenfack, D., Libalah, M., Ngomanda, A., Rossi, V., Sonké, B., Texier, N., & Pélissier, R. (2016). Closing a gap in tropical forest biomass estimation: Taking crown mass variation into account in pantropical allometries. *Biogeosciences*, *13*, 1571–1585. https://doi.org/10.5194/bg-13-1571-2016

Pörtner, H.-O., Roberts, D. C., Poloczanska, E. S., Mintenbeck, K., Tignor, M., Alegría, A., Craig, M., Langsdorf, S., Löschke, S., Möller, V., & others. (2022). *IPCC, 2022: Summary for policymakers*.

R Core Team, R. (2013). *R: A language and environment for statistical computing*.

Raumonen, P., Kaasalainen, M., Åkerblom, M., Kaasalainen, S., Kaartinen, H., Vastaranta, M., Holopainen, M., Disney, M., & Lewis, P. (2013). Fast Automatic Precision Tree Models from Terrestrial Laser Scanner Data. *Remote Sensing*, *5*, 491–520. https://doi.org/10.3390/rs5020491

Richards, G., & Brack, C. (2004). A continental stock and stock change estimation approach for Australia. *Australian Forestry*, *67*. https://doi.org/10.1080/00049158.2004.10674948

Ruxton, G. D. (2014). Why are so many trees hollow? *Biology Letters*, *10*(11), 20140555. https://doi.org/10.1098/rsbl.2014.0555

Sæbø, J. S., Socolar, J. B., Sánchez, E. P., Woodcock, P., Bousfield, C. G., Uribe, C. A. M., Edwards, D. P., & Haugaasen, T. (2022). Ignoring variation in wood density drives substantial bias in biomass estimates across spatial scales. *Environmental Research Letters*, *17*(5), 054002. https://doi.org/10.1088/1748-9326/ac62ae

Schmidt, S., Stewart, G. R., & Ashwath, N. (1999). Monitoring plant physiological characteristics to evaluate mine site revegetation: A case study from the wet-dry tropics of northern Australia. *Plant and Soil*, *215*(1), 73–84. https://doi.org/10.1023/A:1004721330261

Sellin, A. (1994). Sapwood–heartwood proportion related to tree diameter, age, and growth rate in *Piceaabies*. *Canadian Journal of Forest Research*, *24*(5), 1022–1028. https://doi.org/10.1139/x94-133

Sheppard, J., Morhart, C., Hackenberg, J., & Spiecker, H. (2016). Terrestrial laser scanning as a tool for assessing tree growth. *iForest - Biogeosciences and Forestry*, *10*, 172–197. https://doi.org/10.3832/ifor2138-009

Slik, J. W. F., Paoli, G., Mcguire, K., Amaral, I., Barroso, J., Bastian, M., Blanc, L., Bongers, F., Boundja, P., Clark, C., Collins, M., Dauby, G., Ding, Y., Doucet, J. L., Eler, E., Ferreira, L., Forshed, O., Fredriksson, G., Gillet, J. F., … Zweifel, N.

(2013). Large trees drive forest aboveground biomass variation in moist lowland forests across the tropics. *Global Ecology and Biogeography*, *22*(12), 1261–1271. https://doi.org/10.1111/geb.12092

Veldman, J. (2019). Comment on “The global tree restoration potential” | Science. *Science*, *366*. https://www.science.org/doi/full/10.1126/science.aay7976

Wassenberg, M., Chiu, H.-S., Guo, W., & Spiecker, H. (2015). Analysis of wood density profiles of tree stems: Incorporating vertical variations to optimize wood sampling strategies for density and biomass estimations. *Trees*, *29*. https://doi.org/10.1007/s00468-014-1134-7

Werner, P. A., & Murphy, P. G. (2001). Size-specific biomass allocation and water content of above- and below-ground components of three *Eucalyptus* species in a northern Australian savanna. *Australian Journal of Botany*, *49*(2), 155. https://doi.org/10.1071/BT99026

Werner, P. A., & Prior, L. D. (2007). Tree-piping termites and growth and survival of host trees in savanna woodland of north Australia. *Journal of Tropical Ecology*, *23*(6), 611–622. https://doi.org/10.1017/S0266467407004476

Wilkes, P., Shenkin, A., Disney, M., Malhi, Y., Bentley, L. P., & Vicari, M. B. (2021). Terrestrial laser scanning to reconstruct branch architecture from harvested branches. *Methods in Ecology and Evolution*, *12*(12), 2487–2500. https://doi.org/10.1111/2041-210X.13709

Williams, R. J., Zerihun, A., Montagu, K. D., Hoffman, M., Hutley, L. B., & Chen, X. (2005). Allometry for estimating aboveground tree biomass in tropical and subtropical eucalypt woodlands: Towards general predictive equations. *Australian Journal of Botany*, *53*(7), 607. https://doi.org/10.1071/BT04149

Xing, D., Bergeron, J. C., Solarik, K. A., Tomm, B., Macdonald, S. E., Spence, J. R., & He, F. (2019). Challenges in estimating forest biomass: Use of allometric equations for three boreal tree species. *Canadian Journal of Forest Research*, *49*(12), 1613–1622.

Zanne, Amy E., et al. (2009). Data from: Towards a worldwide wood economics spectrum. *Dryad, Dataset*. https://doi.org/10.5061/dryad.234

Zeps, M., Senhofa, S., Zadina, M., Neimane, U., & Jansons, A. (2017). Stem damages caused by heart rot and large poplar borer on hybrid and European aspen. *Forestry Studies*, *66*, 21–26. https://doi.org/10.1515/fsmu-2017-0003

Zobel, B. J., & Jett, J. B. (1995). The Importance of Wood Density (Specific Gravity) and Its Component Parts. In T. E. Timell (Ed.), *Genetics of Wood Production* (pp. 78–97). Springer Berlin Heidelberg. https://doi.org/10.1007/978-3-642-79514-5_4

Zuleta, D., Arellano, G., McMahon, S. M., Aguilar, S., Bunyavejchewin, S., Castaño, N., Chang-Yang, C.-H., Duque, A., Mitre, D., Nasardin, M., Pérez, R., Sun, I.-F., Yao, T. L., Valencia, R., Krishna Moorthy, S. M., Verbeeck, H., & Davies, S. J. (2023). Damage to living trees contributes to almost half of the biomass losses in tropical forests. *Global Change Biology*, *29*(12), 3409–3420. https://doi.org/10.1111/gcb.16687